

Unmanned Aerial Vehicle Based Low Carbon Monitoring Planning

Wen Yi^a, Monty Sutrisna^a, Shuaian Wang^b

^a*School of Engineering and Advanced Technology, College of Sciences, Massey University, Auckland, New Zealand*

^b*Department of Logistics and Maritime Studies, The Hong Kong Polytechnic University, Hung Hom, Hong Kong*

Abstract: Instead of physically visiting all locations of concern by manpower, unmanned aerial vehicles (UAVs) equipped with cameras are a low-cost low-carbon alternative to carry out monitoring tasks. When a UAV flies to conduct monitoring tasks, it does not have to fly at a fixed speed; instead, it should fly at lower speeds over objects of higher concerns and vice versa. This paper addresses the UAV planning problem with a focus on optimizing the speed profile. We propose an infinite-dimensional optimization model for the problem and transform the model into an elegant linear programming formulation based on characteristics of the problem. Finally, we conduct a case study to demonstrate the effectiveness of the proposed model and the efficiency of the proposed solution method.

Keywords: unmanned aerial vehicle; low-carbon logistics; scheduling; infinite-dimensional optimization

25 1 INTRODUCTION

26 Traditionally, there are two methods to monitor an area. The first one is monitoring
27 by patrol agents. This method is very flexible and easy to implement. However, it has
28 two significant drawbacks. The first drawback is that some areas are difficult to access
29 or dangerous, limiting the applicability of monitoring by patrol agents. Another
30 problem is the high manpower costs of safety specialists, especially in developed
31 countries. The second method to monitor is to use video cameras, e.g., at the entrance
32 of residential buildings and at metro stations. Using video cameras can reduce the
33 manpower costs, as a person in a central control room can monitor the scenes in several
34 cameras at the same time. Moreover, video cameras can conduct monitoring tasks on a
35 24/7 basis. A shortcoming of using video cameras is that the locations of video cameras
36 are fixed. Even though some video cameras can rotate and shoot in many directions,
37 they can still only monitor a limited area of a construction site. It is practically
38 impossible to install so many cameras that all corners of a construction site are
39 monitored. By contrast, patrol agents can monitor a much larger area, though not on a
40 24/7 basis. Another drawback of using video cameras is that they can effectively work
41 only with sufficient light in the monitored area.

42 In recent years, using unmanned aerial vehicles (UAVs) that carry video cameras
43 to carry out monitoring tasks integrates the advantages of the above two approaches
44 (Otto et al., 2018). UAVs equipped with cameras can provide a bird-view of locations
45 and acquire image data efficiently, and thus are able to monitor a large area with low

46 manpower costs. Due to these advantages, UAVs, as a low-cost low-carbon alternative
47 to carry out monitoring tasks, have been used in a number of applications. When a
48 natural disaster occurs, UAVs can be used to monitor the affected area and obtain data
49 on the extent of damage (Pi et al., 2020). UAVs can patrol land borders and shorelines
50 between two countries (Kim and Lim, 2018). In agriculture, UAVs can inspect farm
51 conditions for soil and yield analysis (Puri et al., 2017). In build environment, UAVs
52 equipped with infrared imaging are used to monitor the heat transfer of building blocks
53 (Rakha, and Gorodetsky, 2018). In this study, we will develop models to plan a UAV
54 for carrying out monitoring tasks.

55

56 **1.1 Literature review**

57 A building block in UAV routing is obtaining the flying time between two points.
58 Li et al. (2018a) examined a three-dimensional UAV path planning problem in which
59 a UAV travels from one point to another point in an indoor environment while keeping
60 a certain distance from obstacles. They developed A*-based algorithms to identify the
61 shortest path and the path whose height above the floor and stairs is minimized.

62 Some researchers have concentrated on optimizing UAV routes for monitoring a
63 set of nodes, arcs, or an area. In the category on node monitoring, Kim and Lim (2018)
64 proposed a UAV border monitoring concept in which electrification line systems to
65 wirelessly charge drones are deployed. Drones must visit a sequence of nodes
66 considering battery capacity constraints. A mixed-integer linear programming model is

67 developed to determine the locations to install the electrification line systems. Zhen et
68 al. (2019) investigated a routing problem in which UAVs monitor a set of nodes with
69 different accuracy requirements, and in which the height at which a UAV visits each
70 node is optimized as it affects the accuracy level of monitoring. A tabu search
71 metaheuristic approach is developed for the problem. Xia et al. (2019) examined the
72 routing of a fleet of UAVs for monitoring air emissions from a set of vessels (nodes).
73 Different from many routing studies, the vessels are moving rather than standing still.
74 A space-time network model is developed to formulate the problem, which is solved by
75 a Lagrangian relaxation-based method.

76 In some situation UAVs monitor not nodes, but arcs, such as road segments, power
77 transmission lines, and territorial borders. Chow (2016) and Li et al. (2018b) have
78 studied the routing of a fleet of UAVs to monitor vehicle traffic on a set of road
79 segments (arcs) over multiple periods. The problem is formulated as a mixed-integer
80 linear program and solved by approximate dynamic programming in Chow (2016) and
81 a local branching algorithm in Li et al. (2018b). Campbell et al. (2018) pointed out that
82 an arc can be monitored by more than one UAV because UAVs can travel directly
83 between any two points.

84 Some studies have examined the routing of UAVs to monitor an area. Yang et al.
85 (2018) studied the design of a UAV route to monitor a target area with the aim of
86 minimizing the total flying distance. They divided the area into discrete squares, whose
87 side length is small enough to ensure a UAV can monitor a whole square when it flies

88 along its center line. A modified ant colony optimization algorithm is developed to
89 design the UAV route that passes all the discrete squares. Wang et al. (2018) examined
90 the routing of UAVs to monitor disjoint areas over an extended time horizon, in which
91 each area is divided into a number of cells and must be revisited within a time period.
92 The problem is solved by a multiobjective evolutionary algorithm.

93 UAV monitoring planning is also related to the locations of airbases. Vural et al.
94 (2019) considered the problem of determining the locations of airbases of UAVs that
95 are used for surveillance. The functioning of the airbases depends on the weather
96 conditions, which are random by nature. They developed a two-stage stochastic integer
97 linear program to determine the locations of airbases considering uncertainty.

98 Given that UAVs have very limited flying time and distance, vehicles are used to
99 transport and launch UAVs, improving the overall efficiency. Carlsson and Song (2018)
100 examined the coordination between a truck and a UAV. Hu et al. (2019) proposed a
101 vehicle-assisted multiple-drone routing problem and designed a heuristic solution
102 approach.

103 In the above studies, the flying speed of the UAVs is assumed known and constant.
104 We complement these studies by focusing on optimizing the speed of a UAV.

105

106 **1.2 Objectives and contributions**

107 The objective of this research is to propose a model for planning the speed of a
108 UAV to ensure effective monitoring. We consider a UAV that flies along a fixed path

109 and optimize the flying speed of the UAV. The flying speed of the UAV is optimized
110 to ensure that the UAV spends the most time monitoring important segments on the
111 path, subject to constraints that the UAV completes the path without depleting its
112 battery. The contribution of the paper is that we propose an infinite-dimensional
113 optimization model for the problem and transform the model into an elegant linear
114 programming formulation based on characteristics of the problem. The effectiveness of
115 the model is evaluated by numerical experiments.

116 The remainder of the paper is organized as follows: Section 2 describes the
117 problem and formulates an infinite-dimensional optimization model. Section 3
118 proposes a tailored solution method. Section 4 reports the results of a case study.
119 Conclusions are presented in Section 5.

120

121 **2 PROBLEM DESCRIPTION AND OPTIMIZATION MODEL**

122 A UAV flies along a fixed path to monitor an area of interest. We use Figure 1 to
123 illustrate an area of a construction site and use Figure 2 to illustrate the fixed path. The
124 length of the path is L (m), where the starting and ending points are both the depot of
125 the UAV.

126

27
28

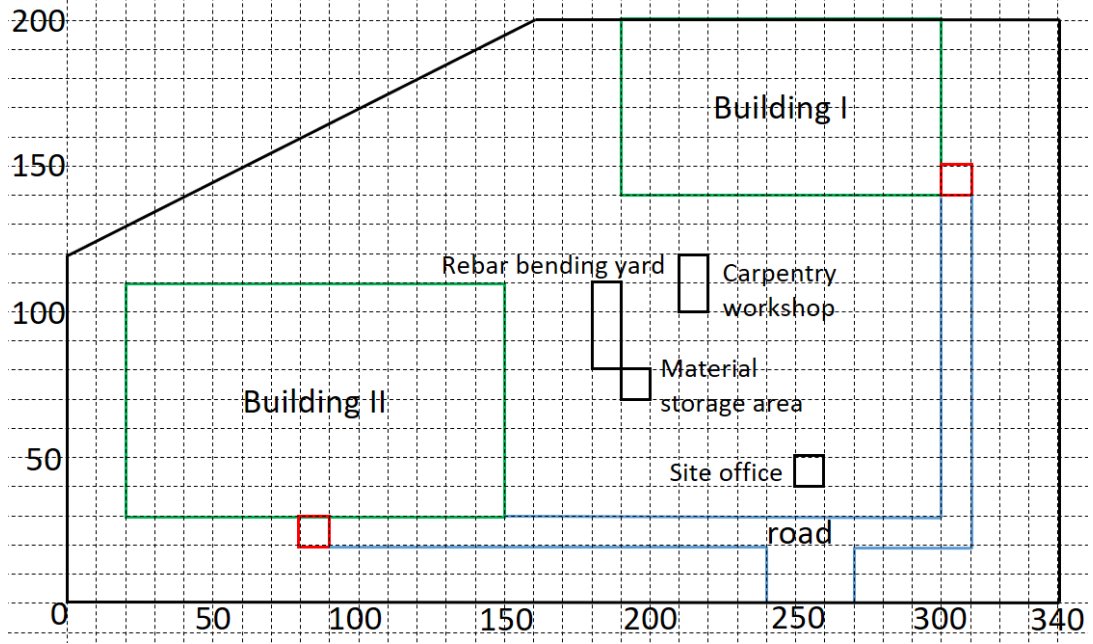


Fig. 1 Layout of a construction site

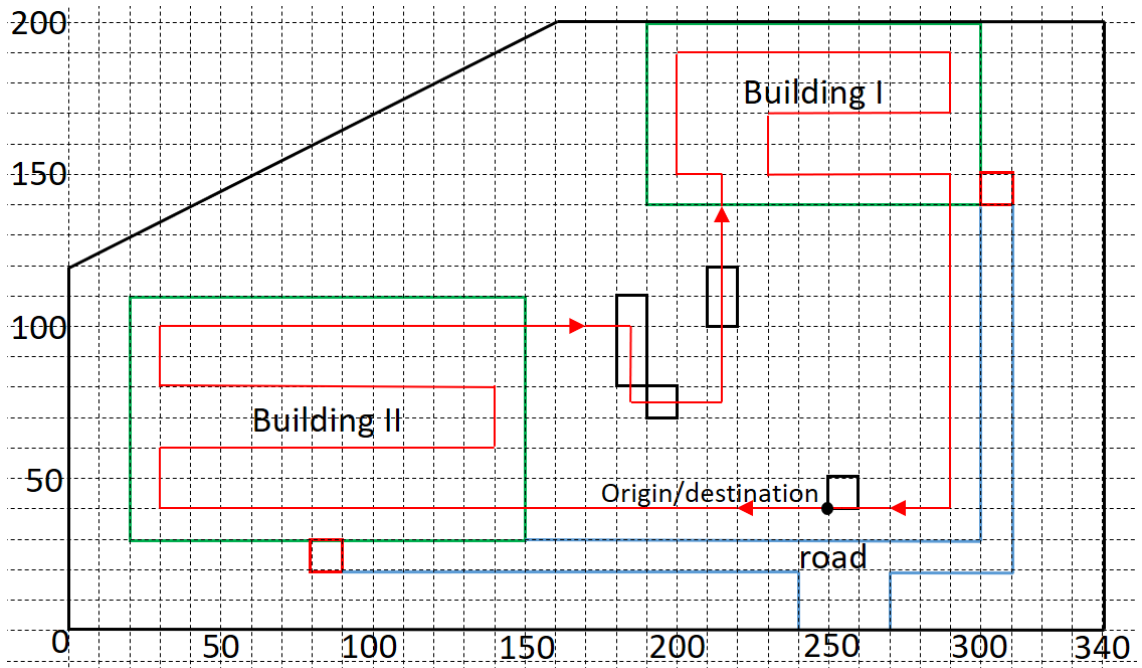


Fig. 2 Flying path of the UAV

134

135

136 The UAV must complete the monitoring tasks along the path in time T (s). The

137 minimum flying speed of the UAV is V^{\min} (m/s) and the maximum flying speed is

138 V^{\max} (m/s). The battery of the UAV has an energy capacity of Q (kWh) and the energy
 139 consumption per meter (kWh/m) when the UAV flies at the speed v (m/s) is denoted
 140 by $F(v)$, $V^{\min} \leq v \leq V^{\max}$. Table 1 shows the flying duration and flying distance of a
 141 type of UAV named “DJI P4 PRO” at different speeds. It can be seen that $F(v)$ is
 142 smaller when v is larger.

143

144 **Table 1** Information on the UAV DJI P4 PRO (Steiner, 2017)

Flying speed (km/h)	Flying duration (min)	Flying distance (km)
5	28	2.3
10	27.5	4.6
15	27	6.8
20	25.5	8.5
25	24	10.0
30	23	11.5
35	22	12.8
40	20	13.3

145

146

147 We denote by y the location on the path that is y (m) away from the origin of the
 148 path. Therefore, the UAV flies from the location $y = 0$ to the location $y = L$. The UAV
 149 can monitor an area with the radius of r (m). That is, when the UAV is at location y ,
 150 $0 \leq y \leq L$, it can monitor the area from location $y - r$ to location $y + r$. Note that in
 151 reality $r \ll L$ and hence we do not need to worry about cases when $y - r < 0$ or $y +$
 152 $r > L$.

153 A location y is monitored when the UAV flies from location $y - r$ to location $y +$
 154 r . Some locations require long duration of surveillance, for example, locations where
 155 workers are conducting dangerous tasks in a construction site, and some locations

156 require minimum surveillance, for example, site offices. Therefore, we define $g(y)$ as
 157 the minimum percentage of time in the T seconds during which location y must be
 158 monitored, $0 \leq y \leq L$. $g(y)$ is specified by site managers and the value of $g(y)$ at
 159 location y is determined by the flying speed of the UAV from $y - r$ to $y + r$.

160 Denote by function $v(y)$ (m/s) the speed function of the UAV that is to be
 161 determined. Represent by $h(y)$ the percentage of time location y is monitored; $h(y) =$
 162 $\frac{1}{T} \int_{y-r}^{y+r} \frac{1}{v(x)} dx$, $0 \leq y \leq L$. It is required that $h(y) \geq g(y)$. We maximize
 163 $\int_0^L g(x)(h(x) - g(x))dx$. In plain words, we maximize the extra surveillance effect
 164 beyond the minimum requirement, that is, $h(x) - g(x)$, weighted by the importance of
 165 the locations, that is, $g(x)$, $0 \leq x \leq L$.

166 The UAV monitoring planning problem with decision functions $v(y)$ and $h(y)$
 167 can be formulated as follows:

$$168 \quad [\text{P1}] \max \int_0^L g(x)(h(x) - g(x))dx \quad (1)$$

169 subject to

$$170 \quad h(y) = \frac{1}{T} \int_{y-r}^{y+r} \frac{1}{v(x)} dx, 0 \leq y \leq L \quad (2)$$

$$171 \quad h(y) \geq g(y), 0 \leq y \leq L \quad (3)$$

$$172 \quad \int_0^L \frac{1}{v(x)} dx \leq T \quad (4)$$

$$173 \quad \int_0^L F(v(x))dx \leq Q \quad (5)$$

$$174 \quad V^{\min} \leq v(y) \leq V^{\max}, 0 \leq y \leq L. \quad (6)$$

175 The objective function (1) maximizes the extra monitoring effect beyond the
 176 minimum requirement weighted by the importance of the locations. Constraint (2)

177 calculates the percentage of time each location is monitored. Constraint (3) enforces the
178 minimum percentage of monitoring time for each location. Constraint (4) requires the
179 UAV to complete the path in time T . Constraint (5) mandates that the energy
180 consumption for the UAV to complete the path is at most Q . Constraint (6) specifies
181 the lower and upper bounds of the flying speeds on the path.

182

183 **3 SOLUTION METHOD**

184 Model [P1] is challenging to solve because its decisions are not scalars or vectors but
185 functions. In other words, model [P1] is an infinite-dimensional optimization problem.
186 Moreover, there are integration operations in the objective function (1) and constraints
187 (2), (4), and (5), which all add to the complexity of the problem. To address the
188 challenges, we examine the properties of the problem and develop a tailored solution
189 method based on these properties.

190

191 **3.1 Reformulation**

192 First, the speed decision $v(y)$ appears in the denominator in constraints (2) and (4),
193 posing difficulty for the problem. We therefore define $t(y) := \frac{1}{v(y)}$ as the new decision
194 function in place of $v(y)$, meaning the flying time (s) per meter at location y , $0 \leq y \leq$
195 L . We further define $f(t(y)) := F(1/t(y))$ as the energy consumption per meter

196 (kWh/m) of the UAV when flying at the speed $1/t(y)$. Then, constraints (2), (4), (5),
 197 and (6) are replaced by the following ones, respectively:

$$198 \quad h(y) = \frac{1}{T} \int_{y-r}^{y+r} t(x) dx, 0 \leq y \leq L \quad (7)$$

$$199 \quad \int_0^L t(x) dx \leq T \quad (8)$$

$$200 \quad \int_0^L f(t(x)) dx \leq Q \quad (9)$$

$$201 \quad \frac{1}{v_{\max}} \leq t(y) \leq \frac{1}{v_{\min}}, 0 \leq y \leq L. \quad (10)$$

202 Second, since $r \ll L$ and a UAV cannot suddenly dramatically change its speed,
 203 $t(x)$ will not change much over $y - r \leq x \leq y + r$. Therefore, constraint (7) can be
 204 approximated by

$$205 \quad h(y) \approx \frac{1}{T} \int_{y-r}^{y+r} t(y) dx = \frac{2r}{T} t(y), 0 \leq y \leq L. \quad (11)$$

206 Embedding Eq. (11) into constraint (3), we have

$$207 \quad t(y) \geq \frac{T}{2r} g(y), 0 \leq y \leq L. \quad (12)$$

208 Combining constraints (10) and (12), we have

$$209 \quad \max\left\{\frac{1}{v_{\max}}, \frac{T}{2r} g(y)\right\} \leq t(y) \leq \frac{1}{v_{\min}}, 0 \leq y \leq L. \quad (13)$$

210 We embed Eq. (11) into the objective function (1) and obtain a new objective function
 211 with decision function $t(y)$:

$$212 \quad [\text{P2}] \max \int_0^L g(x) \left[\frac{2r}{T} t(x) - g(x) \right] dx \quad (14)$$

213 subject to constraints (8), (9), and (13).

214 Model [P2] looks nicer than model [P1] (He, 2016; Tan et al., 2019); however, [P2]
 215 is still an infinite-dimensional optimization problem.

216 **3.2 Discretization**

217 In reality, the function $g(y)$ should be a piecewise constant function. For instance,
 218 when the UAV flies from the origin to Building II in Figure 2, the function $g(y)$ should
 219 be the same constant value; when the UAV flies within the area of Building II, the
 220 function $g(y)$ should be another constant value (we can, of course, divide Building II
 221 into different parts and allow $g(y)$ to have different values for different parts of
 222 Building II). Therefore, we rewrite $g(y)$ as the following form:

223
$$g(y) = g_k, l_{k-1} \leq y \leq l_k, k = 1, \dots, K \quad (15)$$

224 where K is the number of segments that the path is divided into, l_k is a given parameter,
 225 $k = 0, 1, \dots, K, l_0 = 0$ and $l_K = L$. For example, the path in Figure 2 is divided into $K =$
 226 11 segments in Figure 3.

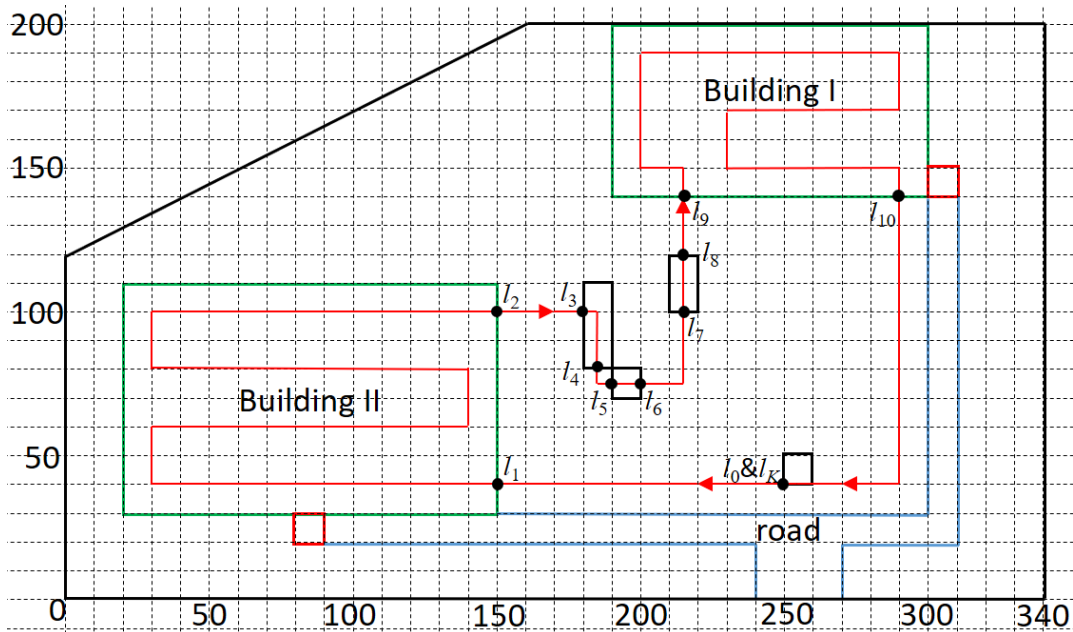


Fig. 3 Divide the path into 11 segments

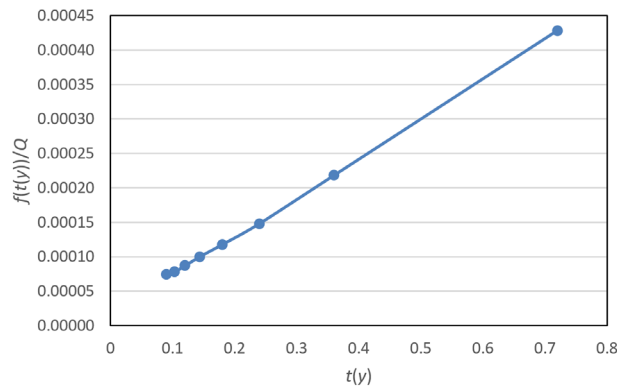
231 Once the path is divided into K segments, a natural question is: is the optimal speed
 232 (equivalently, the optimal $t(y)$) on each segment a constant value or not? To answer
 233 this question, we examine the flying data DJI P4 PRO shown in Table 1. Because we
 234 are concerned with the relation between $t(y)$ (the time required to fly for 1 m) and
 235 $f(t(y))$ (the amount of energy used to fly for 1 m at the speed $1/t(y)$), we plot the
 236 relation in Figure 4 based on the data in Table 1. Note that in Figure 4, the vertical axis
 237 is the $f(t(y))/Q$, that is, the proportion of the total energy capacity of the battery used
 238 to fly for 1 m at the speed $1/t(y)$. In Figure 4, when $t(y) = 0.12$, that is, the speed is
 239 8.33 m/s, or equivalently, 30 km/h, $f(t(y))/Q = 0.00073$. Figure 4 evidently shows
 240 that

241 **Property 1:** $f(t(y))$ is a convex function of $t(y)$.

242 Based on Property 1, we immediately have

243 **Theorem 1:** The optimal $t(y)$, denoted by $t^*(y)$, is a piecewise constant function and
 244 can be represented by

$$245 \quad t^*(y) = t_k^*, l_{k-1} \leq y \leq l_k, k = 1, \dots, K. \quad (16)$$



246

247

Fig. 4 Relation between $t(y)$ and $f(t(y))$

248

249 Based on Theorem 1, model [P2] is equivalent to the following discretized model
 250 with decision variables $t_k, k = 1, \dots, K$:

$$251 \quad [\text{P3}] \max \sum_{k=1}^K g_k (l_k - l_{k-1}) \left(\frac{2r}{T} t_k - g_k \right) \quad (17)$$

252 subject to

$$253 \quad \sum_{k=1}^K (l_k - l_{k-1}) t_k \leq T \quad (18)$$

$$254 \quad \sum_{k=1}^K (l_k - l_{k-1}) f(t_k) \leq Q \quad (19)$$

$$255 \quad \max \left\{ \frac{1}{v_{\max}}, \frac{T}{2r} g_k \right\} \leq t_k \leq \frac{1}{v_{\min}}, k = 1, \dots, K. \quad (20)$$

256 Model [P3] is no longer an infinite-dimensional optimization problem. It has only K
 257 decision variables. A challenge of solving model [P3] is that constraint (19) is nonlinear
 258 as the function $f(t(y))$ is generally nonlinear.

259

260 3.3 Linearization

261 As mentioned in Property 1, $f(t(y))$ is a convex function of $t(y)$. The functional
 262 form for $f(t(y))$ cannot be derived analytically but has to be estimated numerically.

263 We use a piecewise linear function to estimate $f(t(y))$ by connecting all the available
 264 data, as shown in Figure 4. Mathematically, denote by (t^θ, f^θ) the set of data available,
 265 $\theta = 1, \dots, \Theta$. We then estimate $f(t(y))$ as

$$266 \quad f(t(y)) = \max_{\theta=1, \dots, \Theta-1} \left[\frac{f^{\theta+1} - f^\theta}{t^{\theta+1} - t^\theta} (t(y) - t^\theta) + f^\theta \right]. \quad (21)$$

267 Since $f(t(y))$ is estimated as a piecewise linear convex function, we can linearize
 268 constraint (19) by introducing decision variables u_k , $k = 1, \dots, K$, and replace the
 269 nonlinear constraint (19) by the following three groups of linear constraints:

$$270 \quad \sum_{k=1}^K (l_k - l_{k-1}) u_k \leq Q \quad (22)$$

$$271 \quad u_k \geq \frac{f^{\theta+1} - f^\theta}{t^{\theta+1} - t^\theta} (t_k - t^\theta) + f^\theta, \theta = 1, \dots, \Theta - 1, k = 1, \dots, K \quad (23)$$

$$272 \quad u_k \geq 0, k = 1, \dots, K. \quad (24)$$

273 where u_k is the energy consumption per meter (kWh/m) when the UAV flies on
 274 segment $k = 1, \dots, K$.

275 We thus have a linear programming model [P4] with objective function (17) and
 276 constraints (18), (20), (22), (23), and (24). Model [P4] can be solved by off-the-shelf
 277 solvers (Yan et al., 2011; He et al., 2020).

278

279 4 COMPUTATIONAL EXPERIMENTS

280 We carry out a case study to demonstrate the applicability of the proposed model
 281 and algorithm. The layout of the construction site is shown in Figure 1, the path of the
 282 UAV is shown in Figure 2, and the path is divided into 11 segments, as shown in Figure
 283 3. The lengths of the 11 segments are shown in Table 2. Segments 2, 4, 6, 8, and 10
 284 correspond to Building II, rebar bending yard, material storage area, carpentry
 285 workshop, and Building I, respectively. Therefore, these five segments require

286 surveillance by UAV and their minimum percentage of time to be monitored g_k is also
 287 shown in Table 2.

288

289 **Table 2** Information of the 11 segments on the path

Segment	Length	g_k	Note
1	100	0.00	
2	520	0.01	Building II
3	30	0.00	
4	20	0.05	Rebar bending
5	10	0.00	
6	10	0.01	Storage
7	40	0.00	
8	20	0.04	Carpentry
9	20	0.00	
10	325	0.01	Building I
11	140	0.00	

290

291 The UAV is a DJI P4 PRO whose flying parameters are shown in Table 1 and
 292 Figure 4. The other parameters of the UAV are $r = 10$, $V^{\min} = 1$, and $V^{\max} = 40$. The
 293 UAV needs to complete the path in $T = 180$ seconds. The linear programming model
 294 [P4] is solved using CPLEX 12.6.3 on a PC equipped with 3.60GHz of Intel Core i7
 295 CPU and 16GB of RAM.

296 The case is solved to optimality in 0.01s. The optimal objective value is 0.6475. In
 297 the optimal solution, the total flying time (i.e., the left-hand side of constraint (18)) is
 298 exactly 180s.

299 The optimal solutions of t_k and u_k are shown in Table 3. We can see from Table
 300 3 that the solution has a clear structure. Since segment 4 has the largest value of g_k (i.e.,
 301 segment 4 is the most important), the flying speed on it is the lowest (1 km/h). Then,

302 segment 8 is the second most important and the UAV also flies at a low speed on it.

303 The UAV flies at the highest speed on the other segments.

304

305 **Table 3** Optimal solution

Segment	Optimal t_k (s)	Optimal flying speed (km/h)	Optimal u_k
1	0.09	40	0.0001
2	0.09	40	0.0001
3	0.09	40	0.0001
4	3.26	1	0.0019
5	0.09	40	0.0001
6	0.09	40	0.0001
7	0.09	40	0.0001
8	0.36	10	0.0002
9	0.09	40	0.0001
10	0.09	40	0.0001
11	0.09	40	0.0001

306

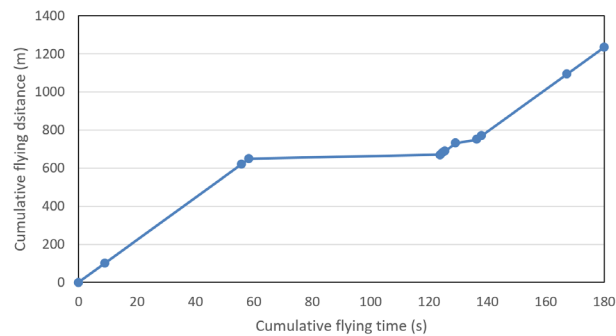
307

308 We further plot the flying-time–flying-distance curve in Figure 5. It can be seen

309 that the UAV spends long time on segment 4. The slopes of the curve, which correspond

310 to the flying speeds, are equal except those on segment 4 and segment 8.

311

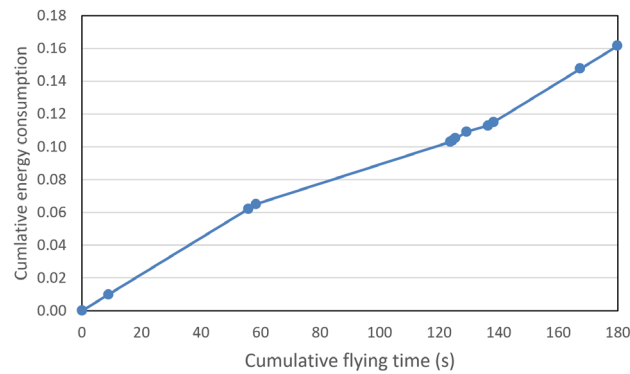


312

313 **Fig. 5** Relation between cumulative flying time and cumulative flying distance

314

315 The flying-time–energy-consumption curve is plotted in Figure 6. It can be seen
 316 that the slopes of the curve, which correspond to the power consumption rates (i.e.,
 317 energy consumption per unit time), are equal except those on segment 4 and segment
 318 8. Note that although the power consumptions per meter on segment 4 and segment 8
 319 are higher than those on the other segments because of the lower speeds on segment 4
 320 and segment 8, the power consumptions per second on segment 4 and segment 8 are
 321 lower than those on the other segments, as shown in Figure 6.
 322



323
 324 **Fig. 6** Relation between cumulative flying time and cumulative energy
 325 consumption
 326
 327

328 5 CONCLUSIONS

329 This study has proposed a UAV monitoring planning problem in which a UAV
 330 flies on a fixed path. The flying speed of the UAV is optimized to ensure that the UAV
 331 spends the most time monitoring important segments of the path while ensuring that
 332 the UAV completes the path within a certain time and without depleting its battery. We
 333 propose an infinite-dimensional optimization model for the problem and transform the

334 model into an elegant linear programming formulation based on characteristics of the
335 problem. A case study is carried out to demonstrate the applicability of the proposed
336 UAV scheduling model. In general, the UAV flies at low speeds on important segments
337 of the path and at its highest speeds on less-important segments.

338

339 **ACKNOWLEDGMENT**

340 This study is supported by Massey University Research Fund (MURF) RM20721.

341

342 **REFERENCES**

343 Campbell, J. F., Corberán, Á., Plana, I., & Sanchis, J. M. (2018). Drone arc routing
344 problems. *Networks*, 72(4), 543-559.

345 Carlsson, J. G., & Song, S. (2018). Coordinated logistics with a truck and a
346 drone. *Management Science*, 64(9), 4052-4069.

347 Chow, J. Y. (2016). Dynamic UAV-based traffic monitoring under uncertainty as a
348 stochastic arc-inventory routing policy. *International Journal of Transportation
349 Science and Technology*, 5(3), 167-185.

350 He, J. (2016). Berth allocation and quay crane assignment in a container terminal for
351 the trade-off between time-saving and energy-saving. *Advanced Engineering
352 Informatics*, 30(3), 390-405.

353 He, J., Tan, C., Yan, W., Huang, W., Liu, M., & Yu, H. (2020). Two-stage stochastic
354 programming model for generating container yard template under uncertainty and
355 traffic congestion. *Advanced Engineering Informatics*, 43, 101032.

356 Hu, M., Liu, W., Peng, K., Ma, X., Cheng, W., Liu, J., & Li, B. (2018). Joint routing
357 and scheduling for vehicle-assisted multidrone surveillance. *IEEE Internet of
358 Things Journal*, 6(2), 1781-1790.

359 Kim, S. J., & Lim, G. J. (2018). Drone-aided border surveillance with an electrification
360 line battery charging system. *Journal of Intelligent & Robotic Systems*, 92(3-4),
361 657-670.

362 Li, F., Zlatanova, S., Koopman, M., Bai, X., & Diakit , A. (2018a). Universal path
363 planning for an indoor drone. *Automation in Construction*, 95, 275-283.

364 Li, M., Zhen, L., Wang, S., Lv, W., & Qu, X. (2018b). Unmanned aerial vehicle
365 scheduling problem for traffic monitoring. *Computers & Industrial Engineering*,
366 122, 15-23.

367 Otto, A., Agatz, N., Campbell, J., Golden, B., & Pesch, E. (2018). Optimization
368 approaches for civil applications of unmanned aerial vehicles (UAVs) or aerial
369 drones: A survey. *Networks*, 72(4), 411-458.

370 Pi, Y., Nath, N. D., & Behzadan, A. H. (2020). Convolutional neural networks for
371 object detection in aerial imagery for disaster response and recovery. *Advanced
372 Engineering Informatics*, 43, 101009.

373 Puri, V., Nayyar, A., & Raja, L. (2017). Agriculture drones: A modern breakthrough in
374 precision agriculture. *Journal of Statistics and Management Systems*, 20(4), 507-
375 518.

376 Rakha, T., & Gorodetsky, A. (2018). Review of Unmanned Aerial System (UAS)
377 applications in the built environment: Towards automated building inspection
378 procedures using drones. *Automation in Construction*, 93, 252-264.

379 Steiner, E., 2017. Drone flight stats. [https://airdata.com/blog/2017/UAV-flight-stats-](https://airdata.com/blog/2017/UAV-flight-stats-part-1)
380 [part-1](https://airdata.com/blog/2017/UAV-flight-stats-part-1). Accessed 21 Jun 2020.

381 Tan, C., He, J., & Yu, H. (2019). Mathematical modeling of yard template regeneration
382 for multiple container terminals. *Advanced Engineering Informatics*, 40, 58-68.

383 Vural, D., Dell, R. F., & Kose, E. (2019). Locating unmanned aircraft systems for
384 multiple missions under different weather conditions. *Operational Research*, 1-20.

385 Wang, Y., Kirubarajan, T., Tharmarasa, R., Jassemi-Zargani, R., & Kashyap, N. (2018).
386 Multiperiod coverage path planning and scheduling for airborne
387 surveillance. *IEEE Transactions on Aerospace and Electronic Systems*, 54(5),
388 2257-2273.

389 Xia, J., Wang, K., & Wang, S. (2019). Drone scheduling to monitor vessels in emission
390 control areas. *Transportation Research Part B: Methodological*, 119, 174-196.

391 Yan, W., Huang, Y., Chang, D., & He, J. (2011). An investigation into knowledge-
392 based yard crane scheduling for container terminals. *Advanced Engineering*
393 *Informatics*, 25(3), 462-471.

- 394 Yang, C. H., Tsai, M. H., Kang, S. C., & Hung, C. Y. (2018). UAV path planning
395 method for digital terrain model reconstruction—A debris fan example. *Automation
396 in Construction*, 93, 214-230.
- 397 Zhen, L., Li, M., Laporte, G., & Wang, W. (2019). A vehicle routing problem arising
398 in unmanned aerial monitoring. *Computers & Operations Research*, 105, 1-11.
- 399